CrystEngComm

Structural Changes in Coordination Polymers in Response to Small Changes in Steric Bulk (H vs. Me): An Experimental and Theoretical Study

Journal:	*CrystEngComm*
Manuscript ID	CE-ART-05-2018-000744.R1
Article Type:	Paper
Date Submitted by the Author:	30-May-2018
Complete List of Authors:	Kyratzis, Nicholas; Monash University, School of Chemistry Cao, Winnie; Monash University, School of Chemistry Pas, Ekaterina; Monash University, School of Chemistry Turner, David; Monash University, School of Chemistry

SCHOLARONE™
Manuscripts

Please do not adjust margins

Journal Name

ARTICLE

Structural Changes in Coordination Polymers in Response to Small Changes in Steric Bulk (H *vs.* Me): An Experimental and Theoretical Study

Received 00th January 20xx,
Accepted 00th January 20xx

DOI: 10.1039/x0xx00000x

www.rsc.org/

Nicholas Kyratzis,[a] Winnie Cao,[a] Ekaterina I. Izgorodina[a] and David R. Turner[a*]

Changing the steric bulk on amino-acid substitued naphthalenediimide ligands is shown to dramatically alter their coordination chemistry by changing the preferred conformation of the ligand and hence the structural motifs that assemble. Naphthalenediimide ligands subsituted by glycine (GlyNDI) and aminoisobutyric acid (ibaNDI) have been investigated and contrasted to previous studies using analogous NDI ligands containing chiral amino acids (ααNDIs). Whilst coordination polymers containing ααNDIs form reproducible M_2L_2 metallomacrocyclic motifs, the materials reported here do not, despite only a small change in the steric bulk of the α-carbon substituents. Changing from N-CHR-CO_2^- terminii (for ααNDIs) to N-CH_2-CO_2^- (GlyNDI) or N-CMe_2-CO_2^- (ibaNDI) acts to reduce or increase the steric bulk immediately around the α-carbon, respectively. Seven coordination polymers containing GlyNDI (**1**-**7**) indicate a preference for the ligands to be closely packed in a parallel manner, and three coordination polymers containing ibaNDI (**8**-**10**) show interactions occuring between the NDI cores in a more perpendicular manner; none display the same motif that is observed for the vast majority of previously reported ααNDI-based materials. The reported GlyNDI and ibaNDI coordination polymers include attempts to force formation of macrocycles by forming rotaxane or catenane motifs using co-ligands. Computational studies, and structural comparisons, show that GlyNDI, ibaNDI and ααNDIs adopt different conformations of the carboxylate groups with respect to the NDI core, with the crystallographically observed conformations matching minimised geometries. These conformational differences are a property of the molecule and are not enforced by solid-state packing, showing that small steric changes can have subtle effects on molecular geometry that are observed as pronounced effects in crystal engineering. The previously used ααNDI ligands are therefore shown to have steric demands that are neither too great nor too small, and therefore occupy a 'Goldilocks zone' for the formation of a macrocyclic motif.

Introduction

The concept of deliberately designing coordination polymers and controlling of their topology by judicious selection of organic and inorganic components was first postulated in the late 1980s by Robson and Hoskins.[1] The field has increased almost exponentially since this seminal report. Deliberately engineering coordination frameworks, and as well as organic crystalline materials, for a designed function is rapidly becoming semi-predictable through the application of robust supramolecular synthons.[2] Porous coordination polymers, or metal-organic frameworks,[3] have received particular attention for the range of potential properties that they may possess.[1c] Whilst the role of many supramolecular interactions in coordination-based systems can be 'predicted' to some extent, due largely to their directionality and complementary nature, the role played by steric effects can be harder to forecast.[4] Even subtle changes in bulk can cause significant differences in the products that are obtained and alter the stability of supramolecular synthons. There are many reports of systems in which steric bulk has been observed to bring about a change in the nature of coordination polymers, and it is impossible to be exhaustive here. For example, steric bulk has been shown to alter the amount of available pore space,[5] prevent interpenetration of networks,[6] modulate the ring size of metallomacrocycles,[7] change the immediate coordination environment around polyoxometallates,[8] and change the architecture of metal-cyanide networks.[9] Even very subtle steric changes, *e.g.* methyl *vs.* ethyl, can result in pronounced changes to structure.[10]

Naphthalenediimides are rigid, planar molecules that have been used extensively in supramolecular systems.[11] Their electron deficient nature and fluorescence properties (particularly when core substituted) are frequently exploited, and their rigidity and large aromatic surface being particularly useful for crystal engineering applications. Our previous research into the coordination chemistry of NDI-based ligands has been focused on chiral dicarboxylates, in which the imide positions are formed from amino acid precursors (collectively referred to herein as ααNDIs).[12] We have reported polymeric complexes containing NDI cores substituted by alanine

[a] School of Chemistry, Monash University, Clayton, Vic 3800, Australia.
Electronic Supplementary Information (ESI) available: Additional crystallographic refinement details, PXRD traces. See DOI: 10.1039/x0xx00000x

This journal is © The Royal Society of Chemistry 20xx

Please do not adjust margins

(AlaNDI),[12a-c] leucine (LeuNDI),[12d] and phenylalanine (PheNDI).[12e] Throughout these reports we have observed the repeated reproducibility of an M_2L_2 macrocyclic motif, regardless of the amino acid side chain that is used. This motif occurs in *ca.* 75% of all structures that we have reported, an exceptional level of reproducibility for a supramolecular motif. Of these structures, 75% display interpenetration involving the macrocycle, through either a self-complementary catenane or through rotaxane formation using dipyridyl coligands (Figure 1). Changing the steric bulk of the side chain affects crystal packing and interpenetration, yet retains the macrocyclic motif. We have very recently reported the same motif in discrete catenanes.[13]

In this current work, we report studies into changing from ligands containing chiral amino acids, to those containing achiral coordinating groups (derived from glycine and aminoisobutyric acid). In addition to being achiral, these ligands have a very different steric bulk on the α-carbon than the ααNDIs which unexpectedly results in very different structural behaviour that is rationalised through computational studies of the ligands.

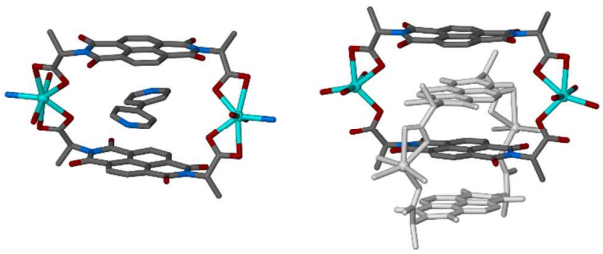

Figure 1. The M_2L_2 macrocyclic motif is observed in 75% of structures we have obtained containing ααNDI ligands, typically forming interpenetrated networks by the formation of π···π driven rotaxane (left) or catenane (right) structures.

Experimental

Materials and Methods

All chemicals and reagents were obtain from commercial sources and were used without purification. H_2glyNDI and H_2ibaNDI were synthesized using literature procedures.[14] FTIR spectra were obtained on an Agilent Cary 630 diamond attenuated total absorbance (ATR) spectrometer using MicroLab software to process the data. Thermogravimetric analyses were conducted using a Mettler TGA/DSC instrument. The temperature was ramped at 5°C min^{-1} to 400°C under an N_2 supply of 10 ml min^{-1}, and data were analysed using the STARe software. Microanalyses were performed at the Science Centre, London Metropolitan University, United Kingdom. Powder X-ray diffraction data were collected at room temperature using a Bruker D8 diffractometer equipped with Cu-Kα radiation (λ = 1.5418 Å). Samples were mounted on a zero background silicon single crystal stage. Data were collected in the angle interval of 2θ = 5-55° with a step size of 0.02°. The collected data were compared to the predicted patterns calculated based on low temperature single crystal data using Mercury (see ESI).[15]

Synthesis

$[Co_4(GlyNDI)_4(DMF)_6(OH_2)_{1.5}]$ (1) and *poly*-$\{(H_2N(CH_3)_2)_2[Co(GlyNDI)_2]\}$ (2Co)

$CoCl_2{\cdot}6H_2O$ (6.7 mg, 28 µmol) and H_2GlyNDI (10 mg, 26 µmol) were placed in DMF (2 mL) in a glass vial and the mixture was sonicated to ensure full dissolution. The solution was heated at 90°C in a dry bath incubator for one week during which time both blue (**2Co**) and green (**1**) plate-like crystals formed, which were collected by vacuum filtration (14.2 mg, 16%). A pure phase of **1** could not be successfully synthesised due to persistent concomitant formation of **2Co** (confirmed by PXRD, see ESI Figure S1), however an alternate synthesis was found to produce only **2** (see below).

***poly*-$[Co_4(GlyNDI)_4(DMF)_6(OH_2)_{1.5}]$ (1)**

$CoCl_2{\cdot}6H_2O$ (62.2 mg, 262 µmol) and H_2GlyNDI (50 mg, 130 µmol) were placed in DMF (10 mL) in a glass vial and the mixture was sonicated to ensure full dissolution. The solution was heated at 120°C in a dry bath incubator for one week during which time green plate-like crystals formed, which were collected by vacuum filtration (72.4 mg, 13%). υ_{max}/cm^{-1}: 3545w, 1713m, 1647m, 1577w, 1452m, 1351m, 1241m, 1008m, 771s. Found C, 48.75; H, 3.44; N, 8.86. $C_{90}H_{77}N_{14}O_{39.5}Co_4$ requires C, 48.64; H, 3.49; N, 8.82%. Phase purity was confirmed by X-ray powder diffraction (see ESI, Figure S2).

***poly*-$[Zn(GlyNDI)(OH_2)_2]{\cdot}0.5H_2O$ (3) and *poly*-$\{(H_2N(CH_3)_2)_2[Zn(GlyNDI)_2]\}$ (2Zn)**

$Zn(NO_3)_2{\cdot}xH_2O$ (15.5 mg, 52 µmol) and H_2GlyNDI (10.0 mg, 26 µmol) were placed in a solvent mixture of DMF (2 mL) and water (1 mL) in a glass vial and the mixture was sonicated to ensure full dissolution. The solution was heated at 90°C in a dry bath incubator for one week, during which time colourless plate-like crystals of **3** and **2Zn** were formed which were collected by vacuum filtration (10 mg). Despite repeated attempts under alternative conditions, neither product could be obtained in isolation (see PXRD in ESI, Figure S3).

***poly*-[Co(GlyNDI)(2,2'-bipy)] (4)**

$CoCl_2{\cdot}4H_2O$ (7.40 mg, 36 µmol), H_2GlyNDI (10 mg, 26 µmol) and 2,2'-bipy (2.5 mg, 16 µmol) were added to DMF (2 mL) in a glass vial and the mixture was sonicated to ensure complete dissolution. The solution was heated at 100°C in a dry bath incubator for one week, during which time purple plate-like crystals of **4** were formed which were collected by vacuum filtration (8.1 mg, 37%). Found C, 56.29; H, 2.72; N, 9.25; $C_{28}H_{16}N_4O_8Co$ requires C, 56.48; H, 2.71; N, 9.41%. υmax (IR) cm-1: 1708s, 1666s, 1493w, 1433m, 1352m, 1242m, 1180m, 1011m, 760m, 732m. Phase purity was confirmed by X-ray powder diffraction (see ESI, Figure S4).

***poly*-[Cu(GlyNDI)(dpe)] (5) and *poly*-$\{(H_2N(CH_3)_2)_2[Cu(GlyNDI)_2]{\cdot}2DMF\}$ (6)**

$CuCl_2$ (8.9mg, 52 µmol), H_2GlyNDI (10mg, 26 µmol) and dipyridylethene (5.0 mg, 27 µmol) were added to a solvent

This journal is © The Royal Society of Chemistry 20xx

mixture of DMF (2 mL), methanol (1 mL) and water (1 mL) in a glass vial and sonicated to ensure full dissolution. The solution was heated at 90°C in a dry bath incubator for one week, during which time both blue (**5**) and green (**6**) plate-like crystals formed, which were collected by vacuum filtration (4.1 mg). Despite many attempts to alter the synthetic conditions, pure phases of **5** and **6** could not be successfully isolated, with PXRD confirming concomitant formation of these two products (see ESI, Figure S5).

***poly*-[Zn(GlyNDI)(dpe)] (7)**

$ZnCl_2 \cdot xH_2O$ (7.1 mg, 52 µmol), H_2GlyNDI (10mg, 26 µmol) and dipyridylethene (4.8 mg, 26 µmol) were added to DMF (2 mL) in a glass vial and sonicated to ensure full dissolution. The solution was heated at 90°C for one week, during which time clear light yellow plate-like crystals were formed, which were collected by vacuum filtration (8.9 mg). PXRD confirms concomitant formation of **2Zn** (see ESI, Figure S6) and a pure sample of **7** could not be isolated.

poly-[Cu(ibaNDI)(DMF)$_2$] (8)

$Cu(NO_3)_2 \cdot xH_2O$ (10.6 mg, 56 µmol), H_2ibaNDI (10 mg, 22 µmol) to DMF (2 mL) in a glass vial and sonicated to ensure full dissolution. The solution was heated at 100°C for one week, during which time green/blue plate-like crystals of **8** were formed, which were collected by vacuum filtration (2.3 mg, 6%). Found C, 50.03; H, 4.52; N, 8.30. $C_{28}H_{30}N_4O_{10}Cu \cdot 1.2H_2O$ requires C, 50.37; H, 4.89; N, 8.39%. υ_{max}/cm^{-1}: 3298w, 2938w, 1711m, 1608m, 1375w, 1319m, 1249m, 1155w, 1098m, 980m, 886m, 704m. TGA showed a mass loss of 22% in the range 80-110°C corresponding to the loss of the two coordinated DMF molecules (calculated 22.6%) followed by the onset of decomposition at 300°C. Phase purity was confirmed by PXRD (see ESI, Figure S7).

***poly*-[Co$_2$(ibaNDI)$_2$(4,4'-bipy)(DMF)$_2$] (9)**

$CoCl_2 \cdot 6H_2O$ (6.9 mg, 0.46 mmol), H_2ibaNDI (10 mg, 0.23 µmol) and 4,4'-bipyridine (2.3 mg, 0.11 µmol) were added to a solvent mixture of DMF (2 mL), MeOH (1 mL) and H_2O (1 mL) in a glass vial and sonicated to ensure full dissolution. The solution was heated at 80°C for one week, during which time purple needle-like crystals of **9** were formed, which were collected by vacuum filtration (15 mg, 80%). Found C, 55.48; H, 4.34; N, 8.52. $C_{60}H_{54}N_8O_{18}Co_2$ requires C, 55.73; H, 4.21; N, 8.67%. υ_{max}/cm^{-1}: 1712m, 1610m, 1460w, 1318s, 1249m, 1155m, 1099m, 883m, 772s. TGA shows no mass loss until the onset of decomposition at *ca.* 300°C. Phase purity was confirmed by PXRD (see ESI, Figure S8).

***poly*-[Cu$_2$(ibaNDI)$_2$(H$_2$ibaNDI)(2,2'-bipy)$_2$] (10)**

$CuCl_2$ (6.9 mg, 40 µmol), H_2ibaNDI (10 mg, 22 µmol) and 2,2'-bipyridine (2.3 mg, 14 µmol) were added to a solvent mixture of DMF (2 mL) and MeOH (1 mL) in a glass vial and sonicated to ensure full dissolution. The solution was heated at 80°C for one week, during which time blue/green plate-like crystals of **10** were formed, which were collected by vacuum filtration (1.43 mg, 4%). Found C, 56.02; H, 3.85; N, 8.15. $C_{86}H_{66}N_{10}CuO_{24} \cdot DMF \cdot 4.6H_2O$ requires C, 56.07; H 4.35; N, 8.08%. υ_{max}/cm^{-1}: 1664m, 1629m, 1449m, 1322s, 1247m, 1158m, 1098m, 1019w, 981m, 880m, 776s, 732s. TGA showed minimal mass loss (ca. 2%) between 30-260°C followed by a sharp loss in mass (72%) between 260-350°C which corresponds to decomposition. Phase purity was confirmed by PXRD (see ESI, Figure S9). The single crystal X-ray diffraction data was treated with the SQUEEZE routine of PLATON which suggests voids containing 65 e- (215 Å^3) per formula unit, slightly less than that suggested by the best-fit microanalysis calculation (86 e-). Microanalysis and TGA imply that some lattice solvent is readily lost prior to analysis.

Crystallographic Details

Crystals were mounted on nylon loops using viscous hydrocarbon oil. All data were collected using the MX1 beamline at the Australian Synchrotron operating at 17.4 keV (λ = 0.7108 Å).[16] Data collection was controlled using the BluICE program.[17] Data indexing and integration were conducted using the XDS software package.[18] All structures were solved using SHELXT and refined against F^2 by least-squares methods using SHELXL-2016 and Olex2 as a graphical interface.[19, 20] All non-hydrogen atoms were refined using an anisotropic model. Hydrogen atoms were placed in calculated positions and refined using a riding model with displacement parameters 1.2 or 1.5 times the isotropic equivalent of their carrier atom. All data are deposited with, and available from, the Cambridge Crystallographic Data Centre (www.ccdc.cam.ac.uk).

The structures of **5**, **7** and **10** contained solvent accessible voids and were processed using the SQUEEZE routine of PLATON.[21] Details of additional refinement restraints/issues for all structures are given in the ESI. Crystallographic and refinement data are summarised in Table 1.

Computational Details

Gaussian 09 was used to generate M062X/aug-cc-pVDZ optimised geometries of the glycine, alanine and aminoisobutyrate derivatives of naphthalenemonoimide (as the carboxylate anion) using the experimental configurations as a starting model.[22-24] Relaxed rotational scans around the imide N-C bond were conducted at the M062X/cc-pVDZ level of theory with an increment of 10 degrees. Electronic energies of the rotational scans were improved at the M062X/aug-cc-pVTZ level of theory. The Conductor-like Polarisable Continuum model (CPCM) with ethanol as solvent was used in all calculations to account for long-range intermolecular interactions in the crystal structures.[25]

Geometries of the ligands obtained from crystallographically determined structures (from previously reported materials and those contained herein) were overlayed by least-squares fitting against the computationally-determined optimised structures using PyMOL.[26]

Please do not adjust margins

Table 1. Crystallographic and refinement details for compounds **1**-**10**.

Identification code	**1**	**2Co**	**2Zn**	**3**	**4**	**5** [a]	**6**	**7** [a]	**8**	**9**	**10** [a]
Empirical formula	$C_{90}H_{74}Co_4N_{14}O_{39.5}$	$C_{40}H_{32}CoN_6O_{16}$	$C_{40}H_{32}N_6O_{16}Zn$	$C_{18}H_{11.5}N_2O_{10.25}Zn$	$C_{28}H_{16}CoN_4O_8$	$C_{30}H_{18}CuN_4O_8$	$C_{32}H_{27}CuN_5O_{13}$	$C_{30}H_{18}N_4O_8Zn$	$C_{28}H_{30}CuN_4O_{10}$	$C_{60}H_{54}Co_2N_8O_{18}$	$C_{86}H_{66}Cu_2N_{10}O_{24}$
Formula weight	2222.37	911.64	918.08	485.16	595.38	626.02	753.12	627.85	646.10	1292.96	1750.56
Crystal system	Triclinic	Monoclinic	Monoclinic	Monoclinic	Monoclinic	Triclinic	Triclinic	Triclinic	Monoclinic	Orthorhombic	Monoclinic
Space group	*P*-1	*C*2/*c*	*C*2/*c*	*C*2/*c*	$P2_1/c$	*P*-1	*P*-1	*P*-1	*C*2/*c*	*Pbcn*	*C*2/*c*
***a*/Å**	15.060(3)	16.464(3)	16.468(3)	16.827(3)	7.2510(15)	11.713(2)	9.864(2)	9.6690(19)	27.105(5)	26.660(5)	24.330(5)
***b*/Å**	17.240(3)	9.1800(18)	9.1690(18)	28.485(6)	18.380(4)	11.938(2)	13.216(3)	13.649(3)	14.012(3)	7.2720(15)	15.230(3)
***c*/Å**	18.790(4)	25.501(5)	25.512(5)	7.4000(15)	17.791(4)	12.993(3)	13.312(3)	14.082(3)	7.4950(15)	27.642(6)	21.710(4)
***α*/°**	92.09(3)	90	90	90	90	115.19(3)	113.74(3)	109.91(3)	90	90	90
***β*/°**	100.49(3)	101.94(3)	102.04(3)	90.71(3)	92.74(3)	105.01(3)	98.29(3)	106.20(3)	94.37(3)	90	97.09(3)
***γ*/°**	115.21(3)	90	90	90	90	96.15(3)	92.58(3)	99.92(3)	90	90	90
Volume/Å^3	4304.1(18)	3770.8(14)	3767.4(14)	3546.7(12)	2368.4(9)	1538.0(7)	1561.7(6)	1602.8(9)	2838.3(10)	5359.0(19)	7983(3)
Temperature/K	100	100	100	100	100	100	100	100	100	100	100
Z	2	4	4	8	4	2	2	2	4	4	4
Refs. collected	128774	28009	31341	28533	42489	58526	57978	60793	13310	56051	109913
Independent refs.	19677	4236	4324	4081	5398	9276	8771	7354	4072	9181	12242
Observed refs. [I>=2σ (I)]	12145	3801	2826	3395	4992	6408	7041	4111	2264	7353	8986
R_{int}	0.1208	0.0447	0.1468	0.1044	0.3037	0.1499	0.0710	2104	0.0978	0.0920	0.1536
GooF	1.007	1.051	1.043	1.079	1.218	1.055	1.039	1.058	1.045	1.032	1.062
R_1 [I>=2σ (I)/all data]	0.0880/0.1250	0.0508/0.0561	0.0901/0.1341	0.0866/0.0977	0.0657/0.682	0.0775/0.1171	0.0684/0.0842	0.0972/0.1466	0.0849/0.1425	0.0781/0.0929	0.0836/0.1113
wR_2 [I>=2σ (I)/all data]	0.2699/0.2352	0.1344/0.1385	0.2220/0.2552	0.2614/0.2687	0.1444/0.1422	0.1915/0.2173	0.1913/0.2073	0.2803/0.3216	0.2502/0.2917	0.2057/0.2171	0.2475/0.2657
CCDC	1840385	1840386	1840387	1840388	1840389	1840390	1840391	1840392	1840393	1840394	1840395

[a] Structures were refined using data processed through the SQUEEZE routine of PLATON.

This journal is © The Royal Society of Chemistry 20xx

Please do not adjust margins

Please do not adjust margins

Results and discussion

Synthesis

Continuing from our previous studies using NDI-based ligands appended by chiral amino acids (alanine, leucine, phenylalanine), we turned our attention to achiral analogues, synthesised using glycine and aminoisobutyric acid. In addition to removing the stereocentres, these ligands (GlyNDI and ibaNDI, see Figure 2) differ from their chiral counterparts by the degree of steric bulk on the α-carbon. In the case of GlyNDI there is reduced steric bulk (two hydrogen atoms on the α-carbon), with the opposite true for ibaNDI (two methyl groups on the α-carbon). Whilst the core functionalities of the ligands remain in place, it is known in crystal engineering that even subtle changes (*i.e.* the addition or removal of a methyl group in these current instances) can have pronounced effects.

The diacids H_2GlyNDI and H_2ibaNDI were readily prepared by condensation reactions between naphthalenetetracarboxylic dianhydride and the corresponding amino acid (see Experimental Details). Coordination polymers were obtained through reactions at elevated, sub-solvothermal temperatures. The ligands were screened under numerous conditions, resulting in eleven coordination polymers being obtained for the two new ligands.

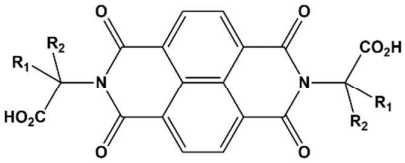

	R_1	R_2
H_2AlaNDI	Me	H
H_2GlyNDI	H	H
H_2ibaNDI	Me	Me

Figure 2. The bis(amino acid) NDIs reported herein and the chiral species, H_2AlaNDI, to which their behaviour is contrasted.

Structural Studies – GlyNDI

The AlaNDI ligand forms polycatenanes involving the metallomacrocyclic motif in coordination polymers without the presence of co-ligands. Initial attempts to explore the behavior of the GlyNDI ligand followed the same approach. The reaction between cobalt(II) chloride and H_2GlyNDI concomitantly formed both green and blue crystals of *poly*-$[Co_4(GlyNDI)_4(DMF)_6(H_2O)_2]$ (**1**) and *poly*-$\{(H_2N(CH_3)_2)_2[Co(GlyNDI)_2)]\}$ (**2Co**), respectively. An alternate synthesis produced **1** in a pure form. **2Co** could not be isolated as a sole product, but an isostructural material (**2Zn**) was the co-product of another reaction (*vide infra*).

poly-$[Co_4(GlyNDI)_4(DMF)_6(H_2O)_2]$ (**1**) is a 2D coordination polymer. Modelled in the triclinic setting *P*-1, the asymmetric unit contains a complete formula unit, with two half occupancy metal atoms situated on inversion centres. All five crystallographically unique Co^{II} ions have octahedral coordination geometries in which four monodentate GlyNDI ligands define an equatorial plane and coordinated solvent occupies the axial positions (either two DMF ligands or H_2O/DMF in the coordination sphere). The 2D sheets consist of Co^{II} chains in which the pairs of neighboring metal ions are bridged by two carboxylates (Figure 3a). Each of the four unique GlyNDI ligands coordinates to four metals (with each of carboxylates bridging two metal ions). Within the 2D sheet, all the GlyNDI ligands are in close proximity and form infinite face-to-face π-stacking chains in the plane of the sheet. The GlyNDI ligands are arranged in an offset, parallel orientation (with respect to the imide N···N vectors). The mean places of adjacent NDI ligands are very slightly non-parallel, with angles in the range 0.69-1.19°. and the closest distances between pairs of carbon atoms in neighbouring NDIs being *ca.* 3.40-3.45 Å. The only noteworthy interactions between the 2D sheets are aromatic CH···O interactions between the NDI cores and imide carbonyl groups.

The connectivity of metals/ligands in the structure of **1** is similar to that observed in many of the previously reported coordination polymers containing the chiral ααNDI ligands. Pairs of ααNDI ligands bridging between monometallic nodes have been shown previously to form macrocycles of the correct size for rotaxane/catenane formation.[12] In the case of **1** however, there appears to be a preference for these ligands to pack closely to each other with coordinating groups of each ligand adopting a *trans* arrangement (with respect to the NDI core). This packing appears to be unfavourable for ααNDI ligands as their steric bulk may prevent the NDIs coming into close proximity with their N···N vectors aligned in a parallel manner.

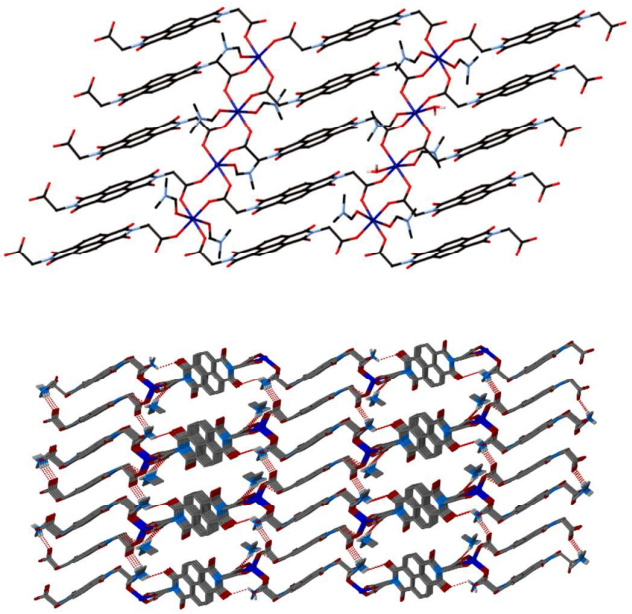

Figure 3. (a) One 2D sheet in the structure of *poly*-$[Co_4(GlyNDI)_4(DMF)_6(H_2O)_{1.5}]$ (**1**) showing the nature of π-stacking between the GlyNDI ligands. (b) The 3D network in *poly*-$\{(H_2N(CH_3)_2)_2[Co(GlyNDI)_2)]\}$ (**2Co**) contains a very similar arrangement of the NDIs to **1** (viewed near the (110) direction). CH hydrogen atoms are omitted for clarity.

Please do not adjust margins

The co-product *poly*-{$(H_2N(CH_3)_2)_2[Co(GlyNDI)_2)]$} (**2Co**) was modelled in the monoclinic setting *C*2/*c* and the asymmetric unit contains half of a formula unit (with halves of two unique GlyNDI ligands). The structure is an anionic 3D coordination polymer that is charge-balanced by dimethylammonium cations (a product of the hydrolysis of DMF used during synthesis). The tetrahedral Co^{II} centres are coordinated by four monodentate GlyNDI ligands resulting in a 3D network in which infinite columns of π-stacking NDIs are arranged in two perpendicular directions (Figure 3b). The NDIs within each stack are not parallel to each other, with the mean planes tilted by *ca.* 4° with respect to their neighbours; the closest C···C distance between adjacent NDI cores is 3.49 Å. The dimethylammonium cations form hydrogen bonds to the GlyNDI ligands; one hydrogen atom interacts solely with one non-coordinated carboxylate oxygen atom whilst the other is bifurcated between a carboxylate and an imide oxygen atom.

The reaction between zinc nitrate and H_2GlyNDI in DMF:H_2O at 90°C also formed two concomitant products, *poly*-$[Zn(GlyNDI)(OH_2)_2]\cdot 0.5H_2O$ (**3**) and *poly*-$\{(H_2N(CH_3)_2)_2[Zn(GlyNDI)_2)]$ (**2Zn**). The structure of **2Zn** is isostructural to **2Co** and is not discussed here. The asymmetric unit of **3** contains one formula unit, with the zinc metal center adopting a distorted trigonal bipyramidal geometry ($\tau = 0.6$)[27] coordinated by three monodentate GlyNDI ligands (one carboxylate being pseudo-chelating with a non-bonding Zn-O distance of 2.53 Å) and two aqua ligands. One of the GlyNDI carboxylate terminii bridges between two metal centers, resulting in a Zn-carboxylate chain parallel to the *c* axis, while the other end binds to a single Zn^{II} and thereby connects the chains into a 3D network (Figure 4).

There are two interpenetrated 3D networks in the structure of **3** (Figure 4c). The individual nets contain no π-interactions within them, with the closest C···C distance being *ca.* 7.1 Å which allows for interpenetration of the second net. The interpenetration results in infinite π-stacked columns parallel to the c axis, with adjacent NDI ligands having an angular offset of 47° (determined from the N···N vectors) and nearest C···C distances of 3.4 Å. The aqua ligands form hydrogen bonds to each other and to imide oxygen atoms, both within and between the individual networks to further stabilise the structure.

Given that the structures of **1**, **2** and **3** formed coordination polymers that display tight packing of the GlyNDI ligands, rather than formation of the anticipated metallomacrocyclic motif, we utilised a capping co-ligand (2,2'-bipyridine) in an attempt to force formation of discrete catenane (seen for some ααNDI ligands).[13] This approach yielded the 1D coordination polymer *poly*-[Co(GlyNDI)(2,2'-bipy)] (**4**), which is a reduction in dimensionality compared to **1**-**3**, due to the inclusion of the capping co-ligand.

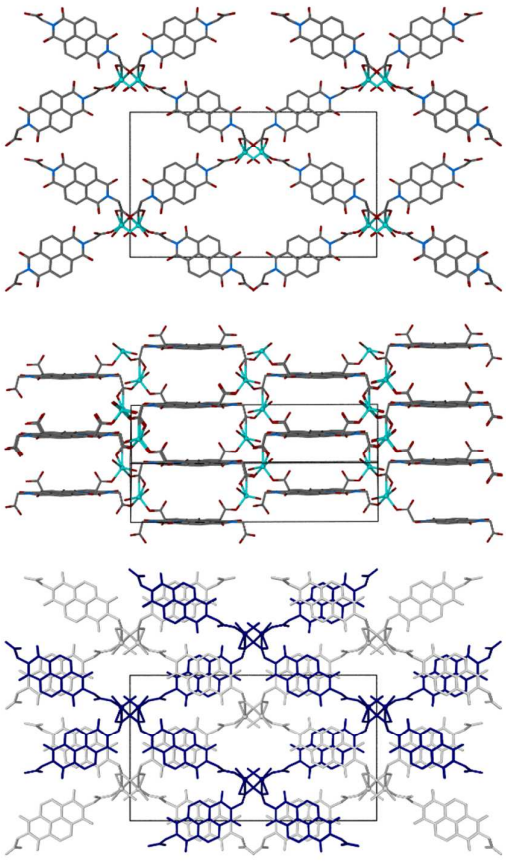

Figure 4. One 3D network in the structure of **3** viewed (a) along the c axis and (b) along the (10-1) direction, highlighting the spacing between the GlyNDI ligands. (c) Two interpenetrating networks showing π-stacking in the c direction.

The asymmetric unit of **4** contains one cobalt metal centre, two halves of GlyNDI ligands and one 2,2'-bipy ligand. The cobalt is six coordinate with two GlyNDI ligands and the 2,2'-bipy ligand all coordinated in a bidentate manner (Figure 5a). The GlyNDI ligands again adopt a *trans* orientation (as in **1**-**3**), the wrong orientation to form the desired macrocyclic motif. The packing of the 1D chains is dominated by π-interactions, with infinite stacks of 2,2'-bipy ligands and of NDI ligands running parallel to the *a* axis (Figure 5b). Antiparallel chains interact *via* the 2,2'-bipy ligands, whilst perpendicular chains interact *via* the NDI cores (note, the propagation directions of the chains are perpendicular, due to their zig-zag nature the NDIs are not exactly perpendicular) with closest C···C contacts in both instances being *ca.* 3.5 Å.

Formation of catenane motifs incorporating the GlyNDI ligand appears not to occur (in the sample size that was obtained) and therefore attempts were made to form rotaxanes by the incorporation of the linear co-ligand 4,4'-dipyridylethene (dpe). Reactions involving Cu^{II} and Zn^{II} yielded two non-interpenetrated materials with the same composition, the 2D coordination polymer *poly*-[Cu(GlyNDI)(dpe)] (**5**) and the 3D network *poly*-[Zn(GlyNDI)(dpe)] (**7**), with concomitant

This journal is © The Royal Society of Chemistry 20xx

formation of *poly*-{$(H_2N(CH_3)_2)_2[Cu(GlyNDI)_2]\cdot 2DMF$} (**6**) and **2Zn**, respectively.

The structure of **5** contains one formula unit in the asymmetric unit, with the square pyramidal copper ($\tau = 0.05$)[27] coordinated by two dpe ligands (*trans* in the basal plane) and three carboxylate groups bound in monodentate fashion. A bimetallic node is formed by one carboxylate atom being in a μ_2 bridging mode. The structure is a (4,4) sheet with the 4-connecting bimetallic nodes being bridged by 'double pillars' (Figure 6), pairs of dpe ligands and pairs of GlyNDI ligands (considering these pairs of ligands as topologically linear connectors, rather than rings). The ligands within these 'double pillars' are engaged in face-to-face π-interactions, with the GlyNDI ligands adopting a similar arrangement to that seen in the structures of **1** and **2** (*i.e.* close-packing with parallel N···N vectors). The windows of adjacent 2D sheets are rotated and slightly offset with respect to each other (with interactions between the NDI ligands of one sheet and the dpe ligands of those directly above/below) and allows for small, solvent-filled 1D channels to exist (overall 18% void space with indeterminate solvent by X-ray diffraction). The connectivity of the coordination polymer **5** is very similar to the previously reported *poly*-[Cd(AlaNDI)(4PyNDI)]·2DMF (where 4PyNDI = bis(4-pyridyl)naphthalenediimide), which also features a 'double pillared' (4,4) topology.[12b] In the latter case however, the AlaNDI ligands form an open macrocycle (*ca.* 7 Å between the NDI cores) whereas the structure of **5** features GlyNDI ligands that are interacting with each other. This suggests that perhaps the change in amino acid is playing a role, with the lower steric hindrance associated with the GlyNDI species allowing the ligands to pack closely together in a parallel manner.

Compound **5** was not able to be isolated in a pure form, always forming concomitantly with *poly*-{$(H_2N(CH_3)_2)_2[Cu(GlyNDI)_2]\cdot 2DMF$} (**6**), confirmed by PXRD (see experimental section). The composition of **6** is similar to that of **2Co**/**2Zn**, containing an anionic framework with dimethylammonium counter cations derived from DMF hydrolysis, but the difference in coordination geometry of the metal yields a very different structure. The 2D anionic $[Cu(GlyNDI)_2]$ network in **6** contains copper paddlewheel nodes, with four GlyNDI ligands forming the paddlewheel motif and two further GlyNDI ligands coordinated to the axial positions of the paddlewheel (Figure 6b). The coordination polymer is a (4,4) sheet, containing π-stacked 'double pillars' similar to those the structure of **5** (again highlighting the persistence of close-packed GlyNDI ligands), and single GlyNDI bridges between the bimetallic nodes. The dimethylammonium cations reside between the layers and form hydrogen bonds to the carboxylate groups in the axial paddlewheel position (pairs of $Me_2NH_2^+$ cations bridge adjacent carboxylates with interactions to both the coordinating and non-coordinating oxygen atoms).

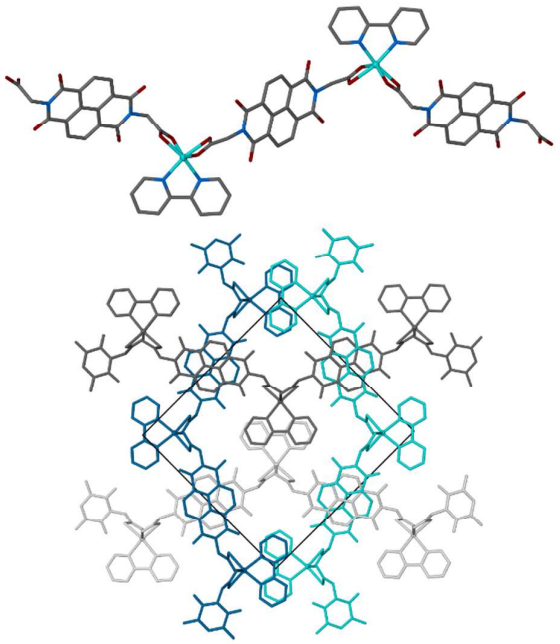

Figure 5. (a)Once chain in the structure of **4**. (b) Packing of the 1D chains (viewed along the *a* axis) ccurs by interactions between the 2,2'-bipy ligands of anti-parallel chains (white/grey and cyan/blue) and by packing of the GlyNDI ligands between perpendicular chains.

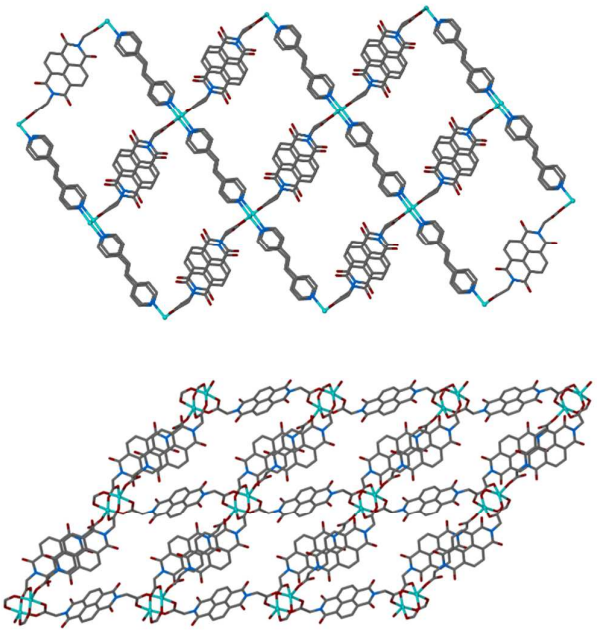

Figure 6. (a) One (4,4) sheet from the structure of **5**, viewed along the 1 0 1 direction, in which there are π-stacked 'double pillars' between the bimetallic nodes. (b) The anionic network in the structure of **6** also contains double GlyNDI bridges between adjacent bimetallic nodes (solvent and counter-cations omitted for clarity).

Poly-[Zn(GlyNDI)(dpe)] (**7**) is a 3D binodal *fsc*-type network containing a 2D sub-structure that is very similar to the 2D

coordination polymer of **1**.[28] The octahedral Zn^{II} centres in **7** are coordinated by four GlyNDIs in an equatorial arrangement, forming metal-carboxylate chains parallel to the *a* axis. The GlyNDI ligands connect these chains into a sheet identical to that in the structure of **1**, with π-stacking of the NDI cores (closest C···C contact 3.4 Å). These sheets are bridged by dpe ligands to form a 3D network; the dpe ligands occupy the axial coordination sites of the metal ions, whereas in the structure of **1** these sites are occupied by DMF ligands. The structure of **7** contains isolated 1D solvent-filled channels (which could not be crystallographically modelled) which account for 26.5% of the unit cell volume (note, gas sorption studies could not be performed due to the concomitant formation of **2Zn**).

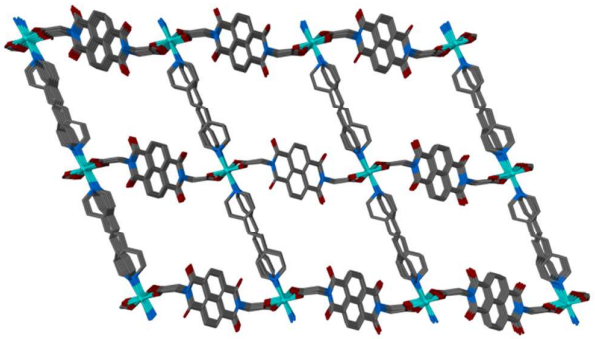

Figure 7. *Poly*-[Zn(GlyNDI)(dpe)] (**7**) is a 3D network that contains a 2D metal-GlyNDI substructure that is identical to that of compound **1** (*c.f.* Figure 3a).

Structural Studies - ibaNDI

Despite a plethora of attempted syntheses using H_2ibaNDI, with and without dipyridyl coligands, only three crystalline materials were able to be isolated and structurally characterised; *poly*-[Cu(ibaNDI)$(DMF)_2$] (**8**), *poly*-[Co_2(ibaNDI)$_2$(4,4'-bipy)$(DMF)_2$] (**9**), and *poly*-[Cu_2(ibaNDI)$_2$(H_2ibaNDI)(2,2'-bipy)$_2$] (**10**). As with the structures derived from H_2GlyNDI, none of these materials contains macrocyclic motifs involving the dicarboxylate although their mode of packing is very different to that in the structures of compounds **1**-**7**.

The asymmetric unit of *poly*-[Cu(ibaNDI)$(DMF)_2$] (**8**) consists of one copper metal centre (residing on an inversion centre), half of an ibaNDI ligand and one coordinated DMF molecule. The copper has a square planar geometry with two monodentate ibaNDI ligands and two DMF molecules coordinated in mutually *trans* positions. The DMF ligands appear engaged in short, yet non-directional CH···O hydrogen bonding to an NDI carbonyl group. The two carboxylate groups of the ibaNDI ligand are situated on opposing sides of the NDI core leading to a 1D coordination polymer (Figure 8a). Adjacent chains interact by π-interactions between the NDI cores with the chains offset by 56° based on the N···N vectors of the NDIs (Figure 8b). The interacting NDIs are near parallel (interplanar angle = 4.5°) and the closest C···C distance between the NDI cores is *ca.* 3.4 Å.

There is a stark difference in behaviour between the ibaNDI ligand, contrasted to both the GlyNDI ligand and the chiral ααNDIs. As with the GlyNDI series the anticipated macrocyclic motif is not formed, the ligand instead adopts the *trans* configuration between monometallic nodes. The π-interactions occur between adjacent NDIs that are oblique, unlike the parallel arrangement of neighbouring NDIs in the structures of **1**, **2**, **5**, **6**, and **7**. It appears that the steric bulk of the two methyl substituents on the α-carbon is too great to allow parallel stacking of the ligands, thereby necessitating interaction at an oblique angle. Further indication of the steric bulk of the isobutyrate substituent comes from distortion of the NDI itself. The NDI core within the ibaNDI ligand deviates from planarity in the structure of **8**, with the nitrogen atoms significantly removed from the plane (analogous to the structures of **9** and **10**, *vide infra*). Using mean plane of the NDI, it is found that the carbon atoms are very close to co-planar (atom···plane distance < 0.08 Å), whilst the oxygen atoms and nitrogen atoms are further removed from this plane (*ca.* 0.25 and 0.19 Å, respectively). Whilst some distortion is observed for the GlyNDI and ααNDI analogues (see later) it is more pronounced for ibaNDI.

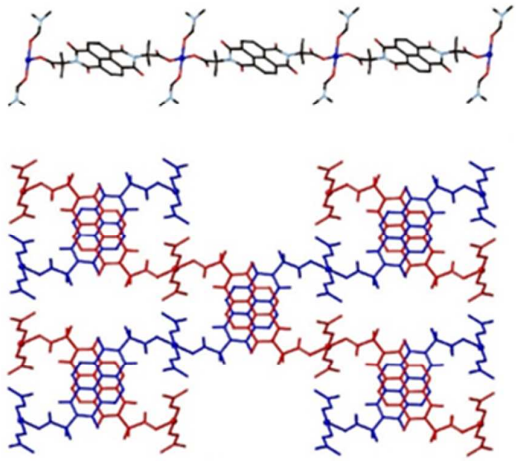

Figure 8. (a) One 1D chain in the structure of *poly*-[Cu(ibaNDI)$(DMF)_2$] (**8**) and (b) stacking of these chains with π interactions between adjacent NDI cores. Hydrogen atoms are omitted for clarity.

Given that the incorporation of dipyridyl ligands in systems containing the ααNDI ligands gave rise to rotaxane motifs, and these motifs were 'allowed' even with the sterically demanding LeuNDI and PheNDI ligands, the same approach was adopted using ibaNDI. The sole crystalline product that was obtained was *poly*-[Co_2(ibaNDI)$_2$(4,4'-bipy)$(DMF)_2$] (**9**). The structure was modelled in the orthorhombic space group *Pbcn*, with the asymmetric unit containing one cobalt(II) ion, one ibaNDI ligand, half of a 4,4'-bipy ligand and a coordinated DMF molecule. The metal centre has a tetrahedral geometry, coordinated by two monodentate ibaNDI ligands, one 4,4'-bipy ligand and a DMF molecule. The ibaNDI and 4,4'-bipy ligands

This journal is © The Royal Society of Chemistry 20xx

are all linear bridges between two adjacent metal ions forming a non-planar (6,3) sheet with the three-connecting Co^{II} nodes (Figure 9a). The structure bears some similarity to that of **8**, with metal-ibaNDI chains, with the carboxylate groups in a *trans* geometry with respect to the NDI core, in the latter instance being bridged by dipyridyl ligands into a network with higher dimensionality. As with the structure of **8**, that of **9** does not display a macrocyclic motif.

The individual (6,3) sheets in the structure of **9** interpenetrate in an inclined 2D→3D manner, with each 6-membered ring of the 2D network being interpenetrated by 4,4'-bipy ligands of three near-perpendicular nets (Figure 9b). The interpenetrated networks form infinite stacks of ibaNDI ligands and of 4,4'-bipy ligands that run parallel to the *b*-axis. The 4,4'-bipy ligands are parallel (interplanar distance 3.14 Å) although they are very offset (centroid···centroid distance 4.41 Å between the closest rings of each pair). The π-stacking NDIs are not parallel (7.24° between the mean planes of adjacent ibaNDI ligands) and have an angle of 60.6° between the N···N vectors of adjacent ligand pairs (*c.f.* compound **9**) and a closest C···C distance of 3.41 Å.

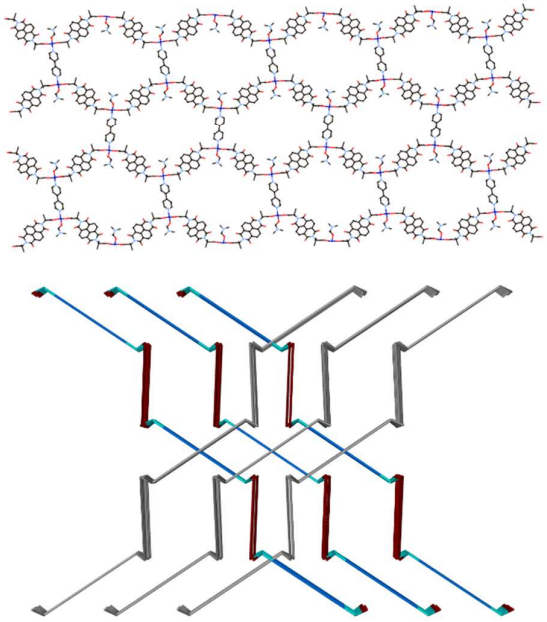

Figure 9. (a) One 2D sheet in the structure of poly-[Co_2(ibaNDI)$_2$(4,4'-bipy)(DMF)$_2$] (**9**) and (b) the 2D→3D inclined interpenetration in which three sheets pass through the windows of one perpendicular sheet (red = ibaNDI, blue = 4,4'-bipy; sheets shown in grey in one direction for clarity).

It is also possible to form discrete metallomacrocycles and catenanes using H_2LeuNDI and capping co-ligands,[13] and this approach was also attempted using H_2ibaNDI in an attempt to force the formation of the desired structural motif. Rather than a discrete complex, the ternary polymeric compound *poly*-[Cu_2(ibaNDI)$_2$(H_2ibaNDI)(2,2'-bipy)$_2$] (**10**) was formed. The structure, modelled in the monoclinic space group *C*2/*c*, contains half of the formula unit in the asymmetric unit. The Cu^{II} centre adopts a distorted square-pyramidal coordination geometry, in which the 2,2'-bipy ligand and two monodentate ibaNDI ligands occupy the basal positions and a monodentate H_2ibaNDI ligand coordinates in the apical position. The coordination environment appears to be distorted due to the presence of a hydrogen bond between the carboxylic acid of the H_2ibaNDI ligand and a non-coordinating carboxylate oxygen atom of an ibaNDI ligand within the coordination sphere (seemingly pushing this ibaNDI ligand below the basal plane). The structure of **10** is a 1D ladder-type coordination polymer in which the ibaNDI ligands comprise the sides of the ladder and the H_2ibaNDI ligands act as the rungs (Figure 10). There are discrete π-stacking interactions in which one H_2ibaNDI is sandwiched between two ibaNDI ligands from adjacent chains, somewhat reminiscent of the metallomacrocycle/guest motif that was the initial aim of this study.

Overall, the ibaNDI-containing structures **8**-**10** all show a similar arrangement between the ligands, with π-stacking occurring between adjacent NDIs that are oriented at an angle to each other (with respect to the N···N vector). This differs from the GlyNDI materials (in which the GlyNDI ligands typically align in a parallel manner) and structures containing the ααNDIs that form a macrocyclic motif in the majority of cases.

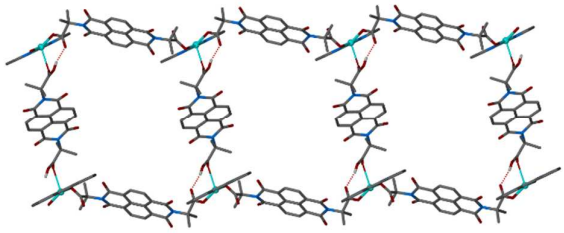

Figure 10. Part of the 1D coordination polymer *poly*-[Cu_2(ibaNDI)$_2$(H_2ibaNDI)(2,2'-bipy)$_2$] (**10**) in which the diacid ligands act as the rungs in the ladder-type structure.

Structural Comparisons and Computational Results

The structural studies of coordination polymers of GlyNDI and ibaNDI make clear that these ligands do not behave in the manner that was anticipated on the basis of our earlier studies using ααNDI ligands.[12] Whilst the sample sizes for GlyNDI/ibaNDI are smaller, the prevalence of a metallomacrocyclic motif from our ααNDI results (around 75% occurrence) suggests that were it a stable motif for these new ligands it would likely have been found. This raises the eternal 'chicken-and-egg' question in crystal engineering as to whether the conformation of the ligand affects crystal packing or vice versa.

In order to determine whether the ligands are intrinsically predisposed to different geometries, despite the relatively small chemical difference between them, computational studies were conducted on analogues of GlyNDI and ibaNDI alongside the closely related AlaNDI (*i.e.* ligands featuring H/H, H/Me or Me/Me substituents on the α-carbon). Optimised geometries were calculated for the analogous naphthalenemonoimides (to minimise computational time)

using a crystallographically-determined geometry as the starting point. This optimised geometry was subsequently confirmed to be the global minimum (*vide infra*) and was used as a basis for RMS fitting of all experimentally determined geometries to produce stacked overlays to compare and contrast the range of observed geometries for the three ligands (Figure 11). Each of the three species shows clustering of the coordinating group within a small range of geometries, in good agreement with the optimised coordinates. Most interestingly, these geometries are quite different from each other, indicating that the steric bulk of the methyl substituents has a significant effect. Relaxed rotational scans around the imide N-αC bond (allowing full relaxation of the remainder of the molecule at each point) confirmed that the optimised structures were global minima. The barriers to rotation were not large (< 40 kJ mol^{-1}) indicating that this bond is free to rotate under the synthetic conditions (see supporting information, Figures S11-S13). Overlays of structures containing PheNDI and LeuNDI are very similar to that of AlaNDI (see Supporting Information),[12d,e] indicating that it is steric bulk immediately adjacent to the α-carbon that is important, rather than more remote steric bulk.

The carboxylate substituent in GlyNDI lies directly 'up' with respect to the NDI core, with the $CHMe(CO_2)$ group staggered with respect to the core. The ibaNDI ligand also adopts a staggered orientation of the $CMe_2(CO_2)$ group, although the carboxylate position is in a different position to that in GlyNDI, now *ca.* 60° rotated. The AlaNDI ligand, with intermediate steric bulk, adopts a conformation mid-way between that of GlyNDI and ibaNDI, with the hydrogen atoms of the α-carbon lying almost co-planar with the NDI core. The influence of steric bulk is also seen in the imide N-αC bond lengths, with an increase in over the GlyNDI<AlaNDI<ibaNDI series from both experimental and predicted results (Table 2) and a more pronounced distortion of the NDI away from planarity with increasing steric bulk (Figure 11). It appears that the geometry of the AlaNDI ligand is ideal for formation of a macrocyclic motif, with the angle between the NDI core and the carboxylate able to set up the geometry required around metal nodes to form macrocycles with the correct NDI···NDI separation for inclusion of guests.

Table 2. Comparison between experimental and calculated bond lengths for the imide C-N bond.

	Average expt. (Å) [a]	Calculated (Å)
GlyNDI	1.465	1.457
AlaNDI	1.485	1.473
ibaNDI	1.505	1.496

[a] Average lengths based on single crystal data from this work (GlyNDI, ibaNDI) or previously published materials (AlaNDI).[12a-c]

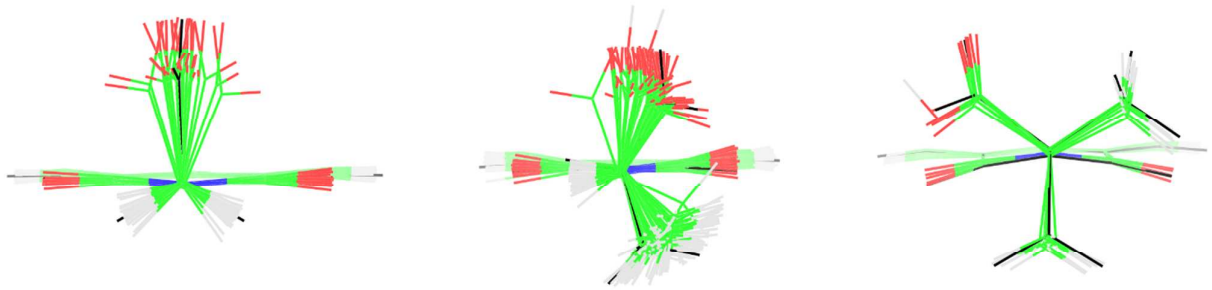

Figure 11. Structural overlays of the terminal imide functionalities from experimental results and geometry optimisations (shown in black) for GlyNDI (left), AlaNDI (centre), and ibaNDI (right) and their free acids, highlighting the close match between the crystallographically observed geometries and the intermediate geometry of AlaNDI contrasted to the more (ibaNDI) and less (GlyNDI) sterically bulky analogues.

Conclusions

Structural analysis of a series of coordination polymers containing GlyNDI or ibaNDI, and comparison of these with structures containing chiral ααNDI ligands, reveals that the chiral ligands occupy a steric sweet-spot – a Goldilocks zone – in which a metallomacrocycle forms, which is not observed for the more (ibaNDI) or less (GlyNDI) sterically bulky ligands. Computational chemistry results confirm that the geometries adopted by the ligands are an intrinsic property, rather than dictated by crystal packing, and thus demonstrates the significant effect arising from an apparently very small change in steric bulk.

Structures containing the GlyNDI ligand (**1**-**7**) show a preference for close packing of the NDI cores in a manner in which the N···N vectors are parallel. Structures containing the ibaNDI ligands (**8**-**10**) again show close packing, but in these instances the NDI cores lie perpendicular to each other. This difference is relatively easy to understand based on the difference in substituents (2 x H vs. 2 x Me) on the α-carbon which affects how the ligands may closest approach each other. Attempts to force the formation of interpenetrated structures, by using dipyridyl coligands, were unsuccessful and yielded only close-packed, non-interpenetrated materials.

Analysis of the optimised geometries reveals very close alignment with experimental results and shows that the AlaNDI conformation is very different to those of GlyNDI and

This journal is © The Royal Society of Chemistry 20xx

ibaNDI. GlyNDI/ibaNDI adopt conformations in which the amino acid group being staggered with respect to the NDI core, to place the most sterically bulky substituents as far as possible from the imide oxygen atoms. The AlaNDI ligand contains two sterically demanding substituents (one carboxylate and one methyl) and therefore the lowest energy conformation places the hydrogen atom in-plane with the NDI core, meaning that the carboxylate is at an intermediate position in comparison to the extremes of GlyNDI and ibaNDI. This conformation gives rise to a robust metallomacrocyclic motif that is not observed for the two achiral ligands.

Conflicts of interest

There are no conflicts to declare.

Acknowledgements

DRT acknowledges the Australian Research Council for funding (FT120100300). Part of this work was conducted using the MX1 beamline at the Australian Synchrotron, part of ANSTO.[16] The authors acknowledge use of facilities within the Monash X-ray Platform.

Notes and references

1 (a) B.F. Hoskins and R. Robson, *J. Am. Chem. Soc.*, 1990, **112**, 1546-1554. (b) R. Robson, *J. Chem. Soc., Dalton Trans.*, 2000, 3735-3744. (c) S.R. Batten, S.M. Neville and D.R. Turner, Coordination polymers: Design, analysis and application, 2009, Royal Society of Chemistry, Cambridge, UK. (d) S. Kitagawa, R. Kitaura and S.-I. Noro, *Angew. Chem. Int. Ed.*, 2004, **43**, 2334-2375.

2 (a) C. Janiak, *Dalton Trans.*, 2003, 2781-2804. (b) A.J. Blake, N.R. Champness, P. Hubberstey, W.S. Li, M.A. Withersby and M. Schroder, *Coord. Chem. Rev.*, 1999, **183**, 117-138. (c) D. Braga, F. Grepioni and G.R. Desiraju, *Chem. Rev.*, 1998, **98**, 1375—405. (d) G.R. Desiraju, *Angew. Chem. Int. Ed.*, 2007, **46**, 8342-8356. (e) G.R. Desiraju, IUCRJ, 2017, 4, 710-711. (f) A.Y. Robin and K.M. Fromm, *Coord. Chem. Rev.*, 2006, **250**, 2127-2157.

3 S.R. Batten, N.R. Champness, X.-M. Chen, J. Garcia-Martinez, S. Kitagawa, L. Öhrström, M. O'Keeffe, M.P. Suh and J. Reedijk, *Pure Appl. Chem.*, 2013, **85**, 1715-1724.

4 (a) B.H. Northrop, Y.-R. Zheng, K.-W. Chi and P.J. Stang, *Acc. Chem. Res.*, 2009, **42**, 1554-1563. (b) E.R.T. Tiekink, *CrystEngComm*, 2003, **5**, 101-113.

5 T. Devic, P. Horcajada, C. Serre, F. Salles, G. Maurin, B. Moulin, D. Heurtaux, G. Clet, A. Vimont, J.-M. Grenèche, B. Le Ouay, F. Moreau, E. Magnier, Y. Filinchuk, J. Marrot, J.-C. Lavalley, M. Daturi and G. Férey, *J. Am. Chem. Soc.*, 2010, **132**, 1127-1136.

6 R. Mondal, M.K. Bhunia and K. Dhara, *CrystEngComm*, 2008, **10**, 1167-1174.

7 R.P. John, K. Lee, B.J. Kim, B.J. Suh, H. Rhee and M.S. Lah, *Inorg. Chem.*, 2005, **44**, 7109-7121.

8 Y.-P. Ren, X.-J. Kong, X.-Y. Hu, M. Sun, L.-S. Long, R.-B. Huang and L.-S. Zheng, *Inorg. Chem.*, 2006, **45**, 4016-4023.

9 E. Colacio, R. Kivekäs, F. Lloret, M. Sunberg, J. Suarez-Varela, M. Bardaji and A. Laguna, *Inorg. Chem.*, 2002, **41**, 5141-5149.

10 (a) T. Wu, R. Zhou and D. Li, *Inorg. Chem. Commun.*, 2006, **9**, 341-345. (b) J.-Q. Liu, Y.-Y. Wang, T. Wu and J. Wu, *CrystEngComm*, 2012, **14**, 2906-2913. (c) S.J. Bullock, F.S. Davidson, R.A. Faulkner, G.M.B. Parkes, C.R. Rice and L. Towns-Andrews, *CrystEngComm*, 2017, **19**, 1273-1278.

11 (a) M. Pan, X.-M. Lin, G.-B. Li and C.-Y. Su, *Coord. Chem. Rev.*, 2011, **255**, 1921-1936. (b) M. Al Kobaisi, S.V. Bhosale, K. Latham, A.M. Raynor and S.V. Bhosale, *Chem. Rev.*, 2016, **116**, 11685-11796. (c) S.V. Bhosale, C.H. Jani and S.J. Langford, *Chem. Soc. Rev.*, 2008, **37**, 331-342. (d) A. Mallick, B. Garai, M.A. Addicoat, P.S. Petkov, T. Heine and R. Banerjee, *Chem. Sci.*, 2015, **6**, 1420-1425.

12 (a) L.J. McCormick and D.R. Turner, *CrystEngComm*, 2013, **15**, 8234-8236. (b) S.A. Boer and D.R. Turner, *CrystEngComm*, 2017, **19**, 2404-2412. (c) S.A. Boer, Y. Nolvachai, C. Kulsing, L.J. McCormick, P.J. Marriott and D.R. Turner, *Chem. Eur. J.*, 2014, **20**, 11308-11312. (d) S.A. Boer, C.S. Hawes and D.R. Turner, *Chem. Commun.*, 2014, **50**, 1125-1127. (e) S.A. Boer and D.R. Turner, *Cryst. Growth Des.*, 2016, **16**, 6294-6303.

13 S.A. Boer, R. Cox, M.J. Beards, H. Wang, W.A. Donald, T.D.M. Bell and D.R. Turner, *Chem. Commun.*, submitted 22/5/18.

14 F.B.L. Cougnon, H.Y. Au-Yeung, G.D. Pantoş and J.K.M. Sanders, *J. Am. Chem. Soc.*, 2011, **133**, 3198-3207.

15 (a) Mercury CSD 3.9, CCDC, Cambridge. (b) C.F. Macrae, P.R. Edgington, P. McCabe, E. Pidcock, G.P. Shields, R. Taylor, M. Towler and J. van de Streek, *J. Appl. Cryst.*, 2006, **39**, 453-457.

16 N.P. Cowieson, D. Aragao, M. Clift, D.J. Ericsson, C. Gee, S.J. Harrop, N. Mudie, S. Panjikar, J.R. Price, A. Riboldi-Tunnicliffe, R. Williamson and T. Caradoc-Davies, *J. Synchrotron Rad.*, 2015, **22**, 187-190.

17 T.M. McPhillips, S.E. McPhillips, H.J. Chiu, A.E. Cohen, A.M. Deacon, P.J. Ellis, E. Garman, A. Gonzalez, N.K. Sauter, R.P. Phizackerley, S.M. Soltis and P. Kuhn, *J. Synchrotron Rad.*, 2002, **9**, 401-406.

18 W. Kabsch, *Acta Cryst.*, 2010, **D66**, 125-132.

19 (a) G.M. Sheldrick, *Acta Cryst.*, 2015, **A71**, 3-8. (b) G.M. Sheldrick, *Acta Cryst.*, 2015, C71, 3-8.

20 O.V. Dolomanov, L.J. Bourhis, R.J. Gildea, J.A.K. Howard and H. Puschmann, *J. Appl. Cryst.*, 2009, **42**, 339-341.

21 (a) A.L. Spek, *Acta Cryst.*, 2009, **D65**, 148-155. (b) A.L. Spek, *Acta Cryst.*, 2015, C71, 9-18.

22 Gaussian 09, Revision A.02, M. J. Frisch, G. W. Trucks, H. B. Schlegel, G. E. Scuseria, M. A. Robb, J. R. Cheeseman, G. Scalmani, V. Barone, G. A. Petersson, H. Nakatsuji, X. Li, M. Caricato, A. Marenich, J. Bloino, B. G. Janesko, R. Gomperts, B. Mennucci, H. P. Hratchian, J. V. Ortiz, A. F. Izmaylov, J. L. Sonnenberg, D. Williams-Young, F. Ding, F. Lipparini, F. Egidi, J. Goings, B. Peng, A. Petrone, T. Henderson, D. Ranasinghe, V. G. Zakrzewski, J. Gao, N. Rega, G. Zheng, W. Liang, M. Hada, M. Ehara, K. Toyota, R. Fukuda, J. Hasegawa, M. Ishida, T. Nakajima, Y. Honda, O. Kitao, H. Nakai, T. Vreven, K. Throssell, J. A. Montgomery, Jr., J. E. Peralta, F. Ogliaro, M. Bearpark, J. J. Heyd, E. Brothers, K. N. Kudin, V. N. Staroverov, T. Keith, R. Kobayashi, J. Normand, K. Raghavachari, A. Rendell, J. C. Burant, S. S. Iyengar, J. Tomasi, M. Cossi, J. M. Millam, M. Klene, C. Adamo, R. Cammi, J. W. Ochterski, R. L. Martin, K. Morokuma, O. Farkas, J. B. Foresman and D. J. Fox, Gaussian, Inc., Wallingford CT, 2016.

23 Y. Zhao and D.G. Truhlar, *Theor. Chem. Acc.*, 2008, **120**, 215-241.

24 (a) T.H. Dunning Jr., *J. Chem. Phys.*, 1989, **90**, 1007-1023. (b) R.A. Kendall, T.H. Dunning Jr. and R.J. Harrison, *J. Chem. Phys.*, 1992, **96**, 6796-6806. (c) D.E. Woon and T.H. Dunning Jr., *J. Chem. Phys.*, 1993, **98**, 1358-1371.

25 (a) V. Barone and M. Cossi, *J. Phys. Chem. A*, 1998, **102**, 1995-2001. (b) M. Cossi, N. Rega, G. Scalmani and V. Barone, *J. Comp. Chem.*, 2003, **24**, 669-681.

26 The PyMOL Molecular Graphics System, Version 2.0 Schrödinger, LLC.

27 A.W. Addison, T.N. Rao, J. Reedijk, J. van Rijn and G.C. Verschoor, *J. Chem. Soc., Dalton Trans.*, 1984, 1349-1356.
28 M. Bi, G. Li, J. Hua, Y. Liu, X. Liu, Y. Hu, Z. Shi and S. Feng, *Cryst. Growth Des.*, 2007, **7**, 2066-2070.

This journal is © The Royal Society of Chemistry 20xx

Structural Changes in Coordination Polymers in Response to Small Changes in Steric Bulk (H *vs.* Me): An Experimental and Theoretical Study

Nicholas Kyratzis,[a] Winnie Cao,[a] Ekaterina I. Izgorodina[a] and David R. Turner[a*]

Table of Contents Entry

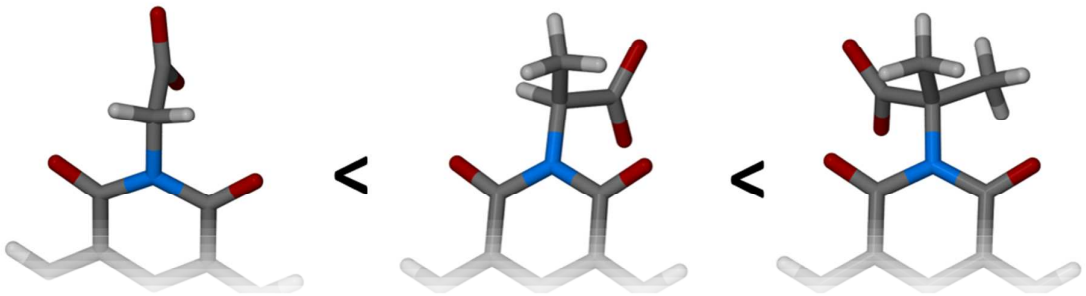

Small changes in the steric bulk in bis(amino acid) naphthalene diimides are shown to have a very significant impact on the structural motifs that are observed in coordination polymers containing the dicarboxylate ligands.